Kinetic inhibition of natural gas hydrates in saline solutions and heptane

ARTICLE *in* FUEL · JANUARY 2014

Impact Factor: 3.52 · DOI: 10.1016/j.fuel.2013.09.012

4 AUTHORS:

Hassan Sharifi
University of British Columbia - Vancouver
11 PUBLICATIONS **40** CITATIONS
SEE PROFILE

John A. Ripmeester
National Research Council Canada
714 PUBLICATIONS **15,661** CITATIONS
SEE PROFILE

Virginia Walker
Queen's University
168 PUBLICATIONS **4,045** CITATIONS
SEE PROFILE

Peter Englezos
University of British Columbia - Vancouver
171 PUBLICATIONS **4,787** CITATIONS
SEE PROFILE

Fuel 117 (2014) 109–117

Contents lists available at ScienceDirect

Fuel

journal homepage: www.elsevier.com/locate/fuel

Kinetic inhibition of natural gas hydrates in saline solutions and heptane

Hassan Sharifi [a], John Ripmeester [b], Virginia K. Walker [c], Peter Englezos [a,*]

[a] Department of Chemical and Biological Engineering, University of British Columbia, Vancouver, British Columbia, Canada
[b] Steacie Institute for Molecular Sciences, National Research Council Canada, Ottawa, Canada
[c] Department of Biology, and School of Environmental Studies, Queens University, Kingston, Ontario, Canada

HIGHLIGHTS

- PVP and PVCap prolonged induction time and reduced growth rate in saline solution.
- Addition of *n*-heptane delayed hydrate nucleation and reduced hydrate growth rate.
- In the presence of heptane, KI addition decreased nucleation time and hydrate growth.
- Gas hydrate dissociated in two steps either in the presence of heptane or without it.

ARTICLE INFO

Article history:
Received 24 July 2013
Received in revised form 4 September 2013
Accepted 6 September 2013
Available online 21 September 2013

Keywords:
Gas hydrate
Kinetic inhibition
Flow assurance
Saline solution
Liquid hydrocarbon

ABSTRACT

The performance of polyvinylpyrrolidone (PVP) and polyvinylcaprolactam (PVCap) as kinetic gas hydrate inhibitors in saline solutions and with heptane was evaluated using high pressure microdifferential scanning calorimetry, as well as with a new apparatus, consisting of two high pressure stainless steel crystallizers. Although PVP and PVCap were found to prolong natural gas hydrate induction time in saline solutions, nucleation was followed by catastrophic hydrate crystal growth. PVP was found to be more effective in this case, since this hydrate growth was modestly slower. The addition of *n*-heptane to the natural gas in the system created a 4th phase. This resulted in increased induction time and a slowing of hydrate growth relative to the gas mixture. Unexpectedly, in the presence of *n*-heptane, addition of kinetic hydrate inhibitors (KHIs) decreased induction time, but catastrophic growth did not occur. Here PVCap was more effective than PVP in both prolonging the induction time and decreasing the rate of hydrate crystal growth. Once formed, however, hydrate decomposition took longer and proceeded in two steps in the presence of *n*-heptane. This observation has profound applications on the use these KHIs under ocean field conditions. In the case of hydrate blockages, our observations that hydrate dissociation started later with the KHIs and complete dissociation took longer could have far reaching economic implications for industry.

1. Introduction

Natural gas hydrates are non-stoichiometric crystalline compounds formed by small size molecules trapped within hydrogen-bonded water cages under low temperature and high pressure conditions [1,2]. Formation of gas hydrates in hydrocarbon transmission pipelines has been identified as a major reason for pipeline blockage [3–5]. Traditionally, gas hydrate formation has been impeded by the injection of thermodynamic hydrate inhibitors (THIs) in order to shift the hydrate phase boundary to higher pressure and lower temperature conditions [6]. However, large amounts of THIs are required to prevent hydrate formation (at an annual estimated cost of $220,000,000) [7] and in addition, safety, health, and environmental risks have pushed industry to seek other inhibitors. Low dosage hydrate inhibitors include kinetic hydrate inhibitors (KHIs) and anti-agglomerates [8–11].

Generally, KHIs are water-soluble polymers which are able to significantly prolong nucleation time and decrease post nucleation crystal growth rates [12]. The key ingredients of successful KHIs are polymers or copolymers containing vinyl-lactam monomers such as pyrrolidone in the form of polyvinylpyrrolidone (PVP) or caprolactam in the form of polyvinylcaprolactam (PVCap) [9]. Although extensive research has been devoted to evaluate the performance of potential KHIs using various techniques [1,13–18], with adsorption-inhibition mechanisms proposed to explain inhibitor action [19–21], their ability to alter gas hydrate crystal nucleation and/or growth is still not understood. In addition, the transferability of kinetic inhibition results between laboratory scale experiments and the field remains a significant challenge [22,23].

* Corresponding author. Address: 2360 East Mall, Vancouver V6T 1Z3, Canada. Tel.: +1 604 822 6184; fax: +1 604 822 6003.
E-mail address: peter.englezos@ubc.ca (P. Englezos).

0016-2361/$ - see front matter © 2013 Elsevier Ltd. All rights reserved.
http://dx.doi.org/10.1016/j.fuel.2013.09.012

In this regard, more recently the performance of the KHIs in the presence of mixture of gases, rather than laboratory-preferred single gas components, have been assessed with a number of techniques (high pressure crystallizers [15,24–26], differential scanning calorimetery [13,16,17], Raman [18,27,28] and ^{1}H NMR spectroscopy [14]) in the hopes of more efficiently moving to field testing. Additional efforts to make such testing even more realistic and relevant for oil and gas reserves, particularly in deep waters, are required. Thus, the impact of parameters such as the salinity and the presence of a hydrocarbon liquid phase need to be assessed. Therefore, in this work a hydrate formation system that better simulates off-shore conditions was selected. These conditions were achieved by (a) employing a multi component (CH_4, C_2H_6, C_3H_8) gas mixture; (b) adding *n*-heptane to model a hydrocarbon liquid phase, and thus represent gas condensate; (c) applying high driving forces (in terms of over pressure or sub-cooling); and (d) increasing water salinity to simulate seawater conditions. In addition, the development of a novel high pressure crystallizer capable of mixing the gas and liquid components resulted in model pipeline conditions on a laboratory scale. A high pressure microdifferential scanning calorimeter (HP-μDSC) was used to evaluate how representative KHIs influence natural gas hydrate formation and dissociation process under these more realistic conditions.

2. Experimental section

2.1. Materials

NaCl (Fisher Scientific) was dissolved in distilled, deionised water to prepare a mass fraction of 3.5% solution. Two commercial KHIs were used: polyvinylpyrrolidone (PVP; average molecular weight of 3.5 kDa; Acros Organics) and a solution (40 wt% in ethanol) of polyvinylcaprolactam (PVCap; average molecular weight of ~23.3 kDa; BASF). The KHIs were diluted to 0.1 mM in the saline solution. A natural gas mixture (UHP grade) consisting of methane (93%)/ethane (5%)/propane (2%) was supplied by Praxair Technology Inc. The liquid hydrocarbon phase was *n*-heptane (Fisher Scientific).

2.2. High pressure crystallizer apparatus

A new high pressure crystallizer was designed and fabricated to conduct gas uptake and dissociation experiments under constant pressure and volume, respectively (Fig. 1). Two 211 mL-stainless steel vessels surrounded by tubing were fitted with two circular polycarbonate viewing windows on the front and back. The vessels contained baffles to control vortex formation when stirred and were submerged in an insulated temperature-controlled circulating bath filled with a propylene glycol and water (1:1) solution. Two additional 300 mL-stainless steel vessels were also immersed in the water bath and acted as supply reservoirs to the crystallizers during hydrate formation. An external refrigerating/heating programmable circulator (VWR Scientific) was used to regulate the temperature of the circulating bath. The contents of the crystallizer were mixed by a gas induced impeller coupled with a hollow shaft which was rotated with a magnetic driven motor (Autoclave Engineers) and controlled by a universal motor controller (Autoclave Engineers). The shaft speed was measured with a universal tachometer display (rpm). Two rosemount smart pressure transmitters (model 3051, maximum uncertainty of 0.075 percent of span 0–15,000 kPa; Norpac controls) were used to measure the pressure of crystallizer and supply vessel and transmit signals to the computer in each unit. Three copper–constantan thermocouples (uncertainty of 0.1 K; Omega Engineering) were used to measure the gas, liquid and interface (liquid–gas, or liquid–liquid) temperature. A high-pressure and low-flow control valve (Fisher, Baumann 5100, NPS ¼) with an actuator and coupled to a proportional, integral, derivative (PID) controller was installed between the crystallizer and the reservoir, and used to regulate crystallizer pressure. The data acquisition system (National Instruments) was connected to a computer to receive transmitted data from pressure transmitters and thermocouples. LabVIEW full development system software (National Instruments) was employed to communicate with the control valve and convert receiving signals for recording into Microsoft Excel.

2.2.1. Gas hydrate crystal formation

In order to simulate pipeline conditions a constant cooling rate method [29,30] using constant pressure was applied. In this procedure, the temperatures of the crystallizers were reduced from outside of the hydrate stability zone to a stable region under constant pressure. Since gas hydrate formation is an exothermic process [1], the onset of nucleation is marked by an abrupt temperature rise and pressure reduction. Two cooling rates (9 K/h and 1 K/h) were employed to simulate both start-up/low flow rate and high flow rate circumstances [31]. The crystallizer was loaded with 80 mL of desired aqueous solution (either saline solution or KHI in saline). Experiments with a liquid hydrocarbon also included *n*-heptane (40 mL) as these KHIs are water soluble polymers [12]; they will remain in aqueous phase in the presence of *n*-heptane. Therefore addition of *n*-heptane does not dilute KHIs solutions. The water bath temperature was adjusted at 293.15 K. The crystallizers were then pressurized so as to achieve conditions below the equilibrium hydrate formation point and subsequently depressurized three times to displace air from the system. After this, the crystallizers were pressurized with gas mixture to 7.0 MPa. The PID controller set point was adjusted at 7.0 MPa to maintain constant crystallizer pressures by the supply of gas from the supply vessels. The supply vessels were pressurized at 10 MPa with the gas mixture. Since the equilibrium hydrate formation temperature in 7.0 MPa is 288.8 K, as calculated by CSMGem [32], no hydrates could form at the initial condition (P = 7.0 MPa, T = 293.15 K). There was constant stirring (500 rpm) of the crystallizer contents and when pressure and temperature were stabilized in both crystallizers and supply vessels, a program of temperature reduction was initiated in order to reach a target temperature of 274.15 K. Refrigeration start time was considered as the zero time and data were recorded every 5 s. The number of moles of gas consumed to form hydrates or dissolved in solution (Δn_H) was calculated as described by Linga et al. [33]. The experiment was terminated when there was a considerable mass of gas hydrate crystals in the crystallizer such that stirring was practically impeded.

2.2.2. Gas hydrate crystal dissociation

Hydrate formation was considered complete when stirring was no longer possible, and thus simulate blocked pipeline conditions. Dissociation of the hydrate crystals was achieved by increasing the water bath temperature from 274.15 K to 301.15 K with similar heating profiles for all experiment. The beginning of the heating program represents time zero in the dissociation experiments. Crystallizer pressures (7.0 MPa at the beginning of hydrate decomposition) increased due to hydrate dissociation and consequent gas expansion. Data were recorded every 5 s. Gas hydrate crystal dissociation initiated once the temperature crossed the equilibrium boundary. The total number of moles of released gas at any given time, Δn_G, was calculated according to Linga et al. [34]. In order to more readily compare different experiments the normalized amount of the released gas was calculated as follows [15]:

$$\text{Normalized amount released gas} = \frac{\Delta n_G}{n_{total}}$$

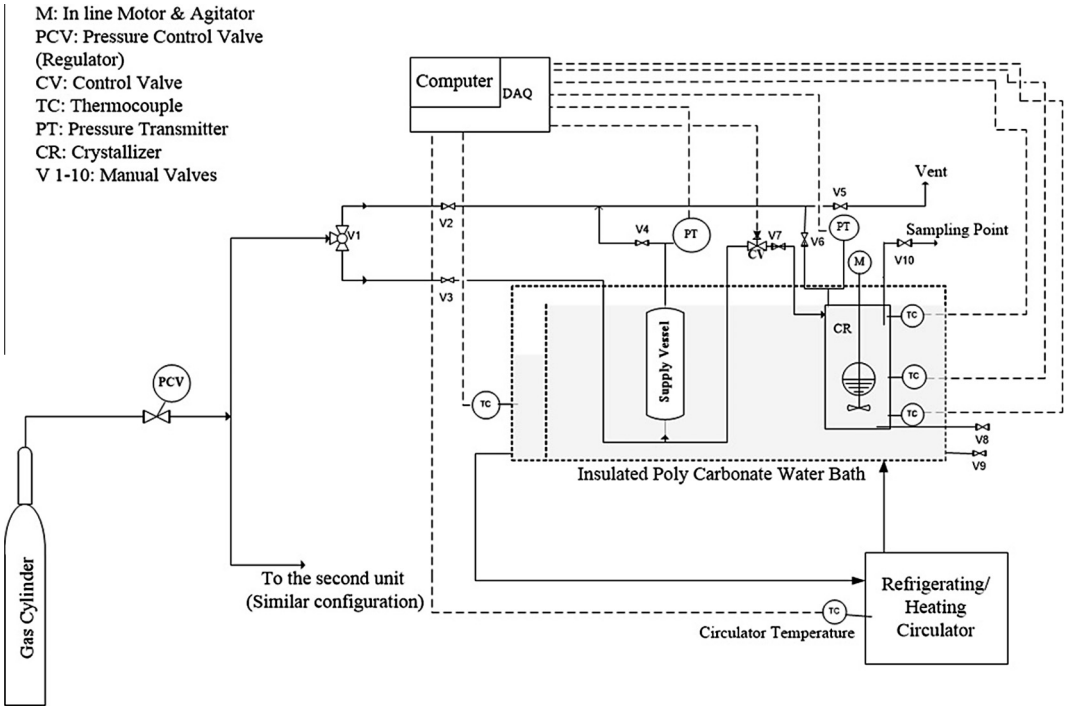

Fig. 1. Schematic of the apparatus. Only one crystallizer and one supply vessel is shown to simplify the diagram.

where n_{total} is the total number of moles of gas recovered at the end of experiment.

2.3. High pressure microdifferential scanning calorimetry (HP-μDSC)

HP-μDSC (μDSC 7 Evo; Setaram Inc.) was used to conduct phase transition experiments. The calorimeter uses double-stage temperature control with Peltier coolers allowing operation between 228.15 K and 393.15 K with a programmable temperature scanning rate (heating and cooling) of 0.001–2 K/min. It consists of two high pressure cells (up to 40 MPa) with volume of 1 mL. A customized "sample holder" was fabricated using stainless steel (316) as shown in Fig. 2. The holder has a base (Dia. 5.4 mm, depth 3.7 mm) with four depressions (Dia. 1.5 mm, depth 2.6 mm), with support from a rod (Dia. 1.6 mm, length 7 mm). Samples (1 μL of the experimental solution with an additional 1 μL *n*-heptane in specific experiments) were injected into the allocated depressions using a micro-syringe, placed in the high pressure cell, and pressurized to 8.0 MPa with the methane/ethane/propane gas mixture. When the sample and reference cell pressure reached the desired value, the temperature ramping program was started. In this protocol, the temperature was decreased from 303.15 K to 243.15 K at a rate of 0.2 K/min to form gas hydrates, and then raised to 303.15 K at the same rate to decompose the formed hydrates. Exothermic peaks represented ice formation, hydrate nucleation and salt precipitation. Eutectic temperature, ice melting and hydrate dissociation were detected by endothermic peaks [13,35]. The identification of ice, precipitated salt and melted ice was facilitated by conducting control experiments with saline solutions at atmospheric pressure. All tank stirred and DSC experiments were repeated three times.

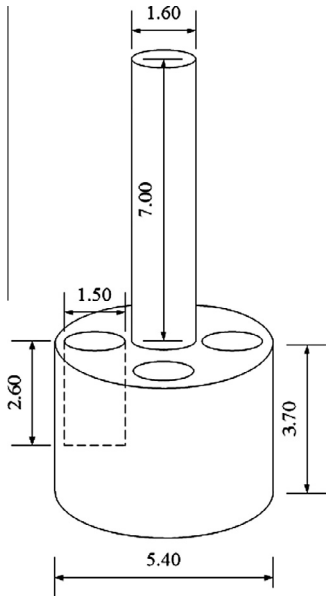

Fig. 2. Sample holder used for DSC experiments (dimensions are in mm; not to scale).

3. Results and discussion

3.1. Gas hydrate nucleation in saline solution

Gas hydrate nucleation is accompanied by a sudden increase in the temperature of the aqueous phase in gas uptake experiments [1,25,36] and in exothermic peaks with DSC [13,16,17] experiments. The increase in temperature also coincides with an increase in gas consumption in gas uptake experiments. In temperature ramping (constant cooling rate) experiments, the lowest temperature that hydrate nucleation occurs is considered as the nucleation temperature [29]. For all experiments the time to nucleation is known as the induction time, with the strength of a KHI assessed by the length of the induction time and the nucleation temperature.

PVP and PVCap were effective inhibitors of gas hydrate formation at two different cooling rates, 9 and 1 K/h (Figs. 3 and

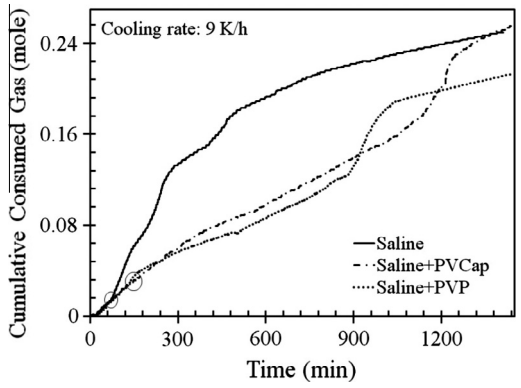

Fig. 3. Typical cumulative gas consumption during hydrate formation in saline solutions with and without inhibitors (PVP or PVCap) with a cooling rate of 9 K/h and P_{exp} = 7.0 MPa. Induction times are: 82.4 min (control), not observed for PVCap, and 151 min (PVP).

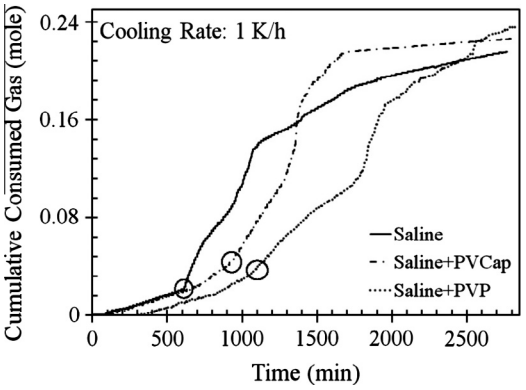

Fig. 4. Typical cumulative gas consumption during hydrate formation in saline solutions with and without inhibitors (PVP or PVCap) with a cooling rate of 1 K/h and P_{exp} = 7.0 MPa. Induction times are: 603.5 min (control), 1049.5 min (PVP), and 959 min (PVCap).

4, respectively). The average induction or hydrate nucleation time was delayed 1.7 and 1.6 times in the presence of PVP and PVCap, respectively (Table 1). Compared to controls, this nucleation occurred at lower temperatures, corresponding to higher sub-cooling (25.2 K for the saline solution *vs.* 29.3 K with PVCap and 32.7 K with PVP). The use of a different cooling rate did not change the relative performance of the two KHIs (Figs. 3 and 4). However, due to a low rate of hydrate formation in the presence of KHIs, the detection of an increase in temperature was more difficult at the higher cooling rate.

The delay in the onset of nucleation due to PVP and PVCap addition in the stirred tank reactor agrees with that observed in

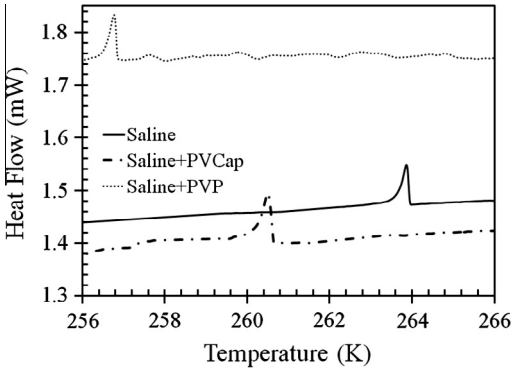

Fig. 5. Typical DSC heating curves showing hydrate nucleation in saline solutions with and without inhibitors (PVP or PVCap).

the HP-μDSC experiments (Fig. 5). Previously, it has been shown that PVP [15,16,18,27] and PVCap [13,26,28] can prolong gas hydrate induction times in water. It was also reported that addition of PVP to a saline solution (artificial seawater) did not increase gas hydrate induction time but promoted gas hydrate growth. On the other hand, the addition of PVCap delayed gas hydrate nucleation and reduced hydrate crystal growth [9]. Here we show that both PVP and PVCap prolong the induction time in saline solution (3.5 wt% NaCl) and nucleation is followed by catastrophic hydrate crystal growth. In our experiments PVP was found to perform better than PVCap in terms of delaying the nucleation of hydrates. This could be attributed to the molecular weight of the PVP used [26,37]. Previously, it was reported that anti-freeze proteins with lower molecular weight than PVCap performed more effective than PVCap in delaying the onset of nucleation [26].

It has been suggested that KHIs can adsorb to hydrate nuclei and/or impurities and thus hinder hydrate nucleation. The evaluation of the relative performance of KHIs is not always clear. Zeng et al. [38] argued that the performance of KHIs was related to the ratio of the dissipation factor, which represents the viscoelastic properties of the adsorbed molecules [39,40], and adsorption mass of KHI. They concluded that the lower ratio, the better performance as KHIs. Further, they argued that PVP molecules preferentially adsorb compared PVCap molecules [38], but the dissipation factor of the adsorbed PVP molecules (with an average molecular weight of 40 kDa for their case) was higher than that of the PVCap molecules. Thus with their reagents PVCap performed more effectively. Dissipation factor is reduced by a decrease in molecular weight of polymers [39]. As a result, the PVP with molecular weight of 3.5 kDa used here would have a lower dissipation factor. Consequently, the ratio of dissipation factor to the adsorbed mass would be lower for this PVP, explaining why this PVP performed more effectively in our experiments.

Table 1
Experimental conditions and results of the gas uptake and DSC experiments showing induction times and nucleation temperatures.

Gas mixture: methane (93%), ethane (5%), propane (2%)	Gas uptake experiments (P_{exp} = 7.0 MPa)				DSC experiments (P_{exp} = 8.0 MPa)	
	Cooling rate: 9 K/h		Cooling rate: 1 K/h			
	Induction time (min)	Nucleation temperature (K)	Induction time (min)	Nucleation temperature (K)	Induction time (min)	Nucleation temperature (K)
Solution						
Saline solution	82.4 ± 0.1	283.5 ± 0.3	603.5 ± 7	283.9 ± 0.1	197.2 ± 2.5	264.5 ± 0.5
Saline + PVP	151 ± 2	275.2 ± 0.1	1049.5 ± 33	276.5 ± 0.5	234.4 ± 1.3	257 ± 0.1
Saline + PVCap	Not observed	Not observed	959 ± 3	278.4 ± 0.1	218.1 ± 1.6	260.4 ± 0.3
Saline + heptane	190.9 ± 3.6	274.2 ± 0.1	1208 ± 4	274.1 ± 0.1	233.7 ± 0.3	257.3 ± 0.1
Saline + PVP + heptane	151.5 ± 0.5	275 ± 0.1	1059 ± 6	276.2 ± 0.1	228 ± 0.6	258.2 ± 0.1
Saline + PVCap + heptane	171.2 ± 0.2	274.2 ± 0.2	1126 ± 2	275.2 ± 0.1	239 ± 0.9	257.6 ± 0.1

3.2. Gas hydrates nucleation in saline solutions and in the presence of a liquid hydrocarbon phase

The results showing induction time and nucleation temperature in the presence of a liquid hydrocarbon (*n*-heptane) are shown in Table 1. The addition of *n*-heptane doubled the induction time (603.5 min to 1208 min, and 82.4 min to 190.9 min in gas uptake experiments). More subcooling was required to form hydrate as seen in the DSC experiments.

Since the equilibrium temperature for the system in the presence of *n*-heptane was 285.6 K at 7.0 MPa, lower than that found in the absence of heptane (288.8 K as seen in Fig. 6), the driving force (T_{eq}–T_{exp}) for hydrate formation with *n*-heptane was also lower. Thus, hydrate appeared to form sooner in the presence of *n*-heptane. However, since hydrate crystals were formed at the interface of aqueous solution and *n*-heptane [41], gas molecules would have to diffuse through the heptane layer in order to reach the surface of the saline solution. Thus the presence of the *n*-heptane layer creates an extra barrier for the transfer of the hydrate forming gas. These two effects (lower equilibrium temperature to form hydrate and an extra mass transfer resistance) resulted in an overall increase in the time required for nucleation.

Unexpectedly, when KHIs and *n*-heptane were added to the crystallizer the induction time was reduced by 20% and 10% for PVP and PVCap, respectively (Figs. 7 and 8). The observation that gas hydrates form sooner in the presence of KHIs in gas uptake experiments has been previously reported [26]. Similar results were obtained in the HP-μDSC experiments (Fig. 9). Clearly, the addition of KHIs to the saline solution in the presence of *n*-heptane modestly increased the nucleation temperature. However, since there is no mixing under the DSC conditions, it is understandable that the difference between nucleation points is not as large as in the gas uptake experiments.

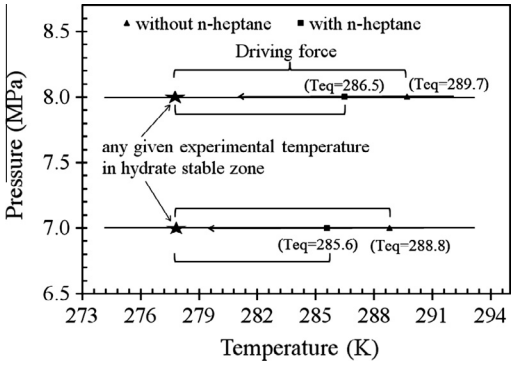

Fig. 6. Calculated gas hydrate equilibrium conditions for the mixture of CH4 (93%), C2H6 (5%), C3H8 (2%) in 3.5 wt% NaCl aqueous solution in the presence of *n*-heptane (squares) or without it (triangles) [32]. At any given experimental temperature, which is shown by star in each curve, driving force (T_{eq}–T_{exp}) in the presence of *n*-heptane was different from that seen in the absence of *n*-heptane.

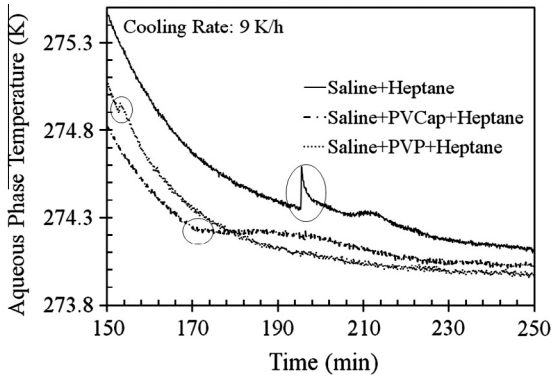

Fig. 7. Effect of KHIs on the induction time in the presence of *n*-heptane in experiments conducted with a 9 K/h cooling rate.

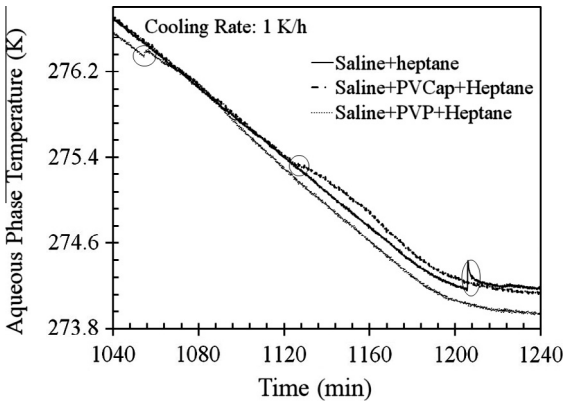

Fig. 8. Effect of KHIs on the induction time in the presence of *n*-heptane in experiments conducted with a 1 K/h cooling rate.

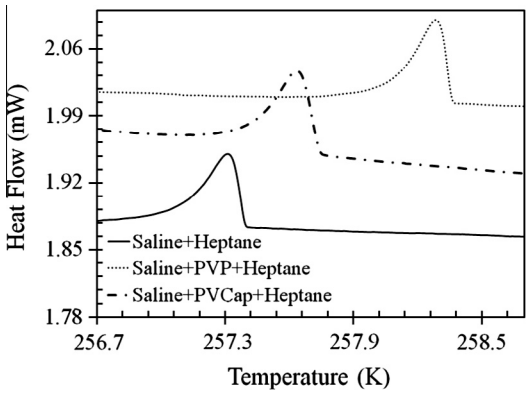

Fig. 9. A typical result using DSC for the effect of PVP and PVCap on nucleation point in the presence of *n*-heptane.

The addition of the KHIs would have decreased the interfacial tension between the aqueous solution and the liquid hydrocarbon [42–44], and the salt served to increase the contact between *n*-heptane and aqueous phase. As a result, the mass transfer between these two phases in hydrate nucleation process increased and thus the hydrate nucleated faster. Under these conditions PVCap performed better than PVP, in contrast to the situation in the absence of *n*-heptane. We speculate that perhaps PVP reduced the interfacial tension between *n*-heptane and saline solution more so than PVCap.

Figs. 10 and 11 show a summary of the mean induction times (with standard deviation) for the different tested solutions in the gas uptake and DSC experiments, which have also been summarized in Table 1. Again, due to a lack of the mixing in the DSC experiments, a comparison in the presence or absence of *n*-heptane was not reasonable.

3.3. Gas hydrate growth

Generally, the addition of KHIs reduced the cumulative gas consumed, reflecting the gas hydrate growth rate in the NaCl (3.5 wt%) solution (Figs. 3 and 4). In the presence of KHIs, hydrate growth proceeded in two steps. In the first phase, growth was correlated with gas consumption (for PVP from induction time at 151 min

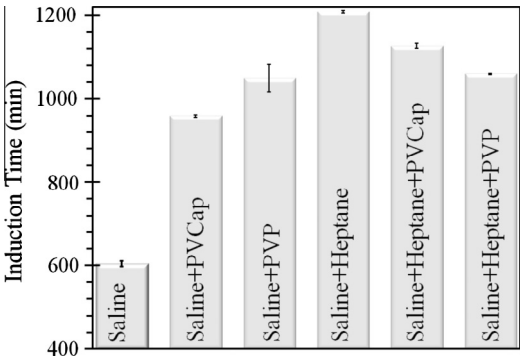

Fig. 10. Effect of KHIs on induction time in saline solution and the presence of *n*-heptane in gas uptake experiments (P = 7.0 MPa, cooling rate: 1 K/h). The means (n = 3) and standard deviations are shown for each condition.

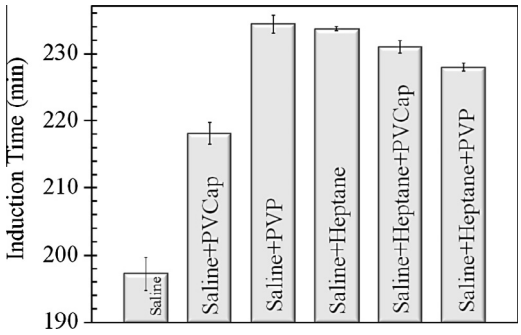

Fig. 11. Effect of KHIs on induction time in saline solution and the presence of *n*-heptane in DSC experiments, P = 8.0 MPa. The means (n = 3) and standard deviations are shown for each condition.

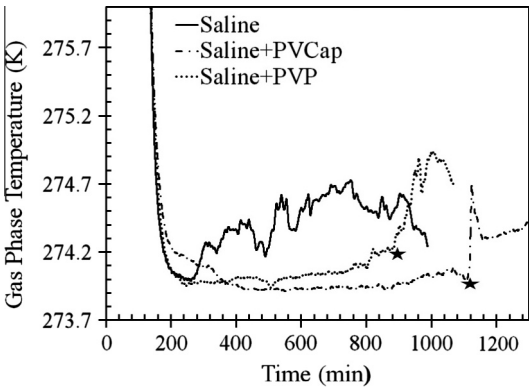

Fig. 12. Gas phase temperatures during gas hydrate formation. The stars indicate the start of the second, rapid phase of growth for the KHI-treatment groups.

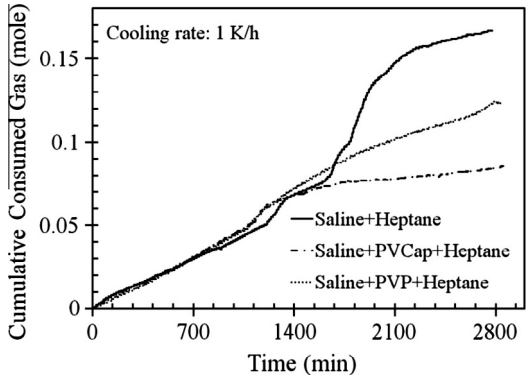

Fig. 13. Effect of PVP and PVCap on cumulative consumed gas in the presence of *n*-heptane in gas uptake experiments (under 1 K/h cooling rate, P = 7.0 MPa).

to 900 min and for PVCap from induction time to 1200 min; Fig. 3). The second phase was catastrophic growth. As shown in Fig. 4, at a cooling rate of 1 K/h in the presence of PVCap, the first phase took 241 min (from induction time at 959 min to 1200 min) with 0.0478 mol gas consumed (0.0002 mol/min), and this was followed by a second phase that was complete in 300 min with 0.1054 mol of gas consumed (0.00035 mol/min). Thus, we suggest that the KHIs regulated growth up to a critical point and after that growth suddenly increased rapidly. Such occurrence in the field would be undesirable. Such catastrophic crystal growth has been previously reported in the absence of saline [41,45]. As hydrate growth proceeded in the first phase, the salt solution would become more concentrated and gas hydrate formation would be reduced due to colligative effects. However, this is less likely to play a role in the catastrophic growth kinetics. PVCap performed better than PVP to inhibit growth initially, as reported [45], but later hydrate formation occurred more rapidly in the presence of PVCap compared to PVP. The rise in the gas phase temperature due to exothermic hydrate formation is consistent with these observations for PVCap (Fig. 12). However, we can only speculate on the reason for catastrophic growth. The higher porosity of the hydrate crystal structure in the presence of kinetic inhibitors [46] may facilitate water transport by capillary action, thereby enhancing gas hydrate formation in the gas phase [46] and resulting in the observed temperature increase (Fig. 12).

Addition of *n*-heptane reduced the rate of hydrate growth. Strikingly, the amount of hydrate formed in the presence of heptane was only 50% of that formed in the absence of this hydrocarbon. As previously discussed, the presence of a heptane layer would provide extra mass transfer resistance for gas diffusion, resulting in a reduced rate of hydrate formation. Both KHIs reduced gas hydrate growth, and in this case, no catastrophic growth was observed (Fig. 13). This inhibition appeared independent of the cooling rate since the same results were obtained at a higher cooling rate (not shown). Since gas hydrate formed on the interface of *n*-heptane and aqueous solution and was situated in the liquid phase, no gas hydrate formed in gas phase in the presence of KHIs. As a result, no catastrophic growth was detected. In this case, the rate of gas hydrate growth in the PVCap experiments was slower than with PVP. For example, in the presence of PVCap, overall hydrate crystallization was reduced 40% while for PVP it was reduced by 28%. Recall that the cooling rate did not affect the performance of PVP and PVCap; they both performed efficiently to control gas hydrate growth at the two tested cooling rates (Figs. 3 and 4).

A summary of the comparisons between the performance of PVP and PVCap in gas hydrate formation under different conditions is presented in Table 2. As it is shown, PVCap performed better in the presence of *n*-heptane, while PVP increased induction time better than PVCap in the saline solution.

Table 2
Comparison between the performance of PVP and PVCap in the formation of gas hydrates under different conditions.

	Hydrate formation mixture	
	Saline solution	Saline + *n*-heptane
To prolong induction time	PVP	PVCap
To decrease growth rate	PVCap	PVCap
To reduce extent of catastrophic growth	PVP	No catastrophic growth was observed

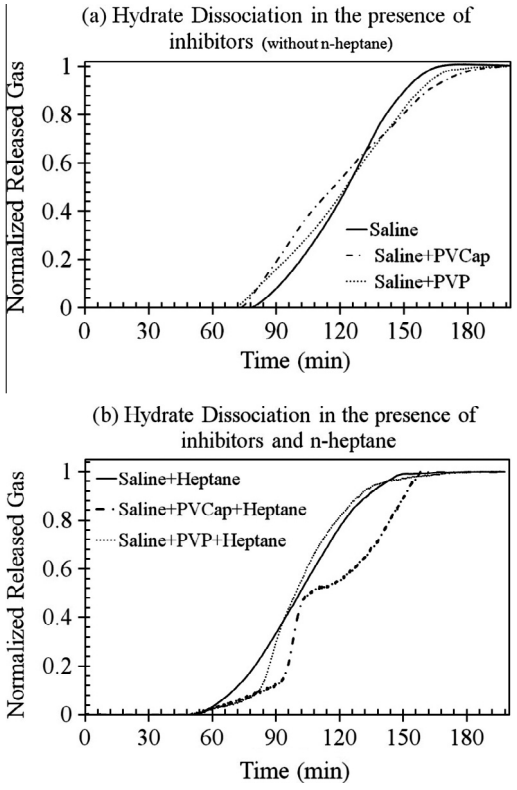

Fig. 14. Effect of PVP and PVCap on gas hydrate dissociation: (a) without heptane and (b) with heptane.

3.4. Gas hydrate dissociation

Once hydrate crystals were formed in the presence of the KHIs, their dissociation was monitored (Fig. 14). Gas hydrates formed in the saline solution started to dissociate earlier but the overall dissociation rate was slower so that in the presence of PVP and PVCap complete dissociation took longer (Fig. 14a). This phenomenon has been observed previously in the absence of salt [15,41]. Adsorption of kinetic inhibitors on the hydrate crystals stabilizes hydrates [47] and hence the hydrate dissociation rate would be lower. Hydrate dissociation in the presence of PVCap was seen to occur in two stages, and we speculate that this two-stage dissociation is related to the presence of different hydrate structures [15]. It is known that the stable hydrate structure for a methane 93%, ethane 5% and propane 2% mixture is sII [48], but both sI and sII of hydrates have been detected in the presence of PVCap [28,49].

The effect of PVP and PVCap on the dissociation process in the presence of *n*-heptane is shown in Fig. 14b. Hydrate dissociation started later, and complete dissociation took longer in the presence of the KHIs. Interestingly, there was an extra step at the initiation of hydrate dissociation in the presence of inhibitors that was not seen in their absence. This suggests that hydrate formed in the presence of KHIs is more stable. Since ethane and propane tend to occupy more hydrate cavities in the presence of kinetic inhibitors [18,27], the methane concentration in the gas phase increases substantively compared to situations in the absence of KHIs. In addition, in the presence of heptanes, the kinetics also reflects the better solubility of propane and ethane in heptane than in methane. In the presence of high methane concentrations in the gas phase, a significantly higher temperature would be required to decompose the hydrates. Added to this situation, there is a sharp increase in the amount of released gas for sII hydrate dissociation (according to CSMGem calculations [32]). In the system with heptane, a two-step decomposition in the presence of PVCap was clearly observed, which we believe is related to the formation of two different hydrate structures (sI and sII). In the first phase, sII hydrate dissociated (CSMGem calculation [32]) and the second section may be related to sI hydrate dissociation. Due to changes in the hydrate dissociation rate in the presence of PVP, such a two-step dissociation mechanism is likely the case but is admittedly not as compelling as that for PVCap.

Since hydrate dissociation is an endothermic process [1], this process can be detected by endothermic peaks in DSC experiments (Fig. 15). In the absence of KHIs, hydrate dissociated at ~ 290 K, equal to the equilibrium value for sII hydrate. In the presence of PVCap, two dissociation peaks appeared (Fig. 15), as has been previously reported [13]. One point (~290 K) is related to sII hydrate (calculated by CSMGem [32]) and the other (293.5 K) cannot be explained. An analogous two-step dissociation was seen and discussed for the autoclave experiments. In the presence of PVP (Fig. 15) there was a broad peak with a minimum at ~291.5 K, whereas with PVCap two minimum points were detected (~290 K and ~292.5 K).

The hydrate equilibrium temperature in the presence of heptane for the gas mixture used in the DSC analysis at 8.0 MPa is 286.5 K (calculated by CSMGem [32]). However, the hydrate dissociated at ~290 K (Fig. 16), which is the equilibrium point without *n*-heptane (Fig. 6). We suggest that due to the lack of the mixing in DSC experiments, the equilibrium point was not affected by *n*-heptane. More peaks were observed in the presence of *n*-heptane than without this hydrocarbon (compare Figs. 15 and 16). Hence, gas hydrate dissociation appears to be more complex in the presence of *n*-heptane, even given the lack of mixing. Integration of endothermic peaks as a function of time during

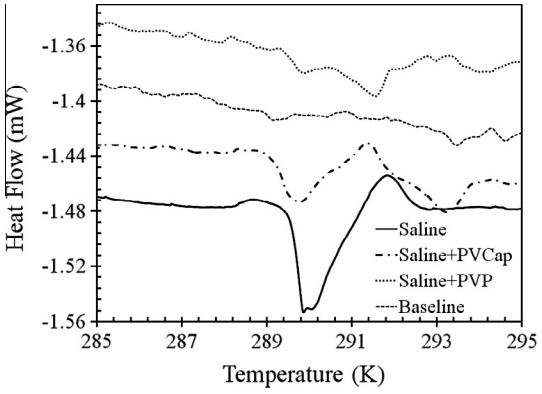

Fig. 15. Typical hydrate dissociation peaks in DSC experiments in the presence of KHIs (P_{exp} = 8.0 MPa, T_{eq} = 289.7 K).

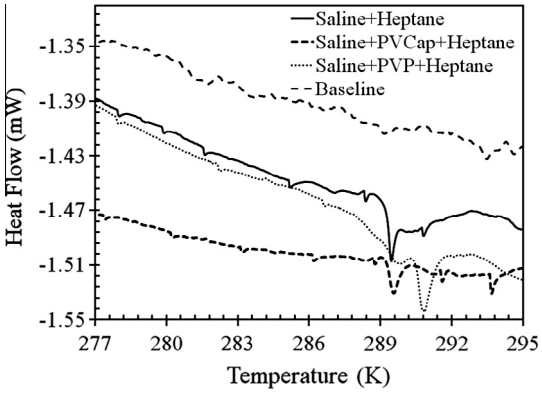

Fig. 16. A typical DSC experiment showing the effect of KHIs on hydrate dissociation peaks in the presence of *n*-heptane (P_{exp} = 8.0 MPa, T_{eq} = 286.5 K).

temperature ramping would show the adsorbed heat in the dissociation process which can be related to the amount of formed hydrate [17]. Calculated mean adsorbed heat (Fig. 16) was 20.18 mj in controls and this was decreased to 8.74 mj and 6.82 mj in the presence of PVP and PVCap, respectively. Hence, the amount of formed hydrate in the presence of *n*-heptane was dramatically reduced by the KHIs: PVP reduced hydrate formation by 56% and PVCap reduced hydrates by 67%. These results have obvious implications for the gas and oil industry.

4. Conclusions

The performance of two KHIs (PVP and PVCap) in the presence of salt and with and without a liquid hydrocarbon was evaluated by monitoring hydrate formation using a set of two identical stirred tank vessels and with calorimetry to determine phase transitions. Under NaCl conditions that mimicked ocean salinity, KHIs significantly prolonged induction time, similar to the effect in a fresh water system. The KHIs were able to regulate hydrate growth following nucleation but only until the point when the rate of gas consumption accelerated rapidly. We refer to this condition as catastrophic growth. PVP (M_w = 3.5 kDa) performed better than PVCap in terms of delaying the nucleation, and catastrophic growth was less severe than that observed in the presence of PVCap. The presence of the KHIs was also useful when initially dissociating the formed hydrates since gas hydrate dissociation started earlier, but complete dissociation took longer in the presence of the inhibitors. We suggest that a two-step dissociation, similar to that seen in fresh water systems, indicated the presence of sI hydrate in addition to the sII hydrate that was expected to form under the prevailing pressure/temperature conditions.

The addition of liquid hydrocarbon to the saline solution was accompanied by an increase in induction time and decrease in growth rate, which we attributed to the fact that the equilibrium temperature in the presence of heptane is lower than without it (3 K lower at 7.0 MPa). In addition, the heptane likely increased the resistance to mass transfer for the hydrate forming gas mixture. Unexpectedly, in the presence of heptane, addition of the inhibitors caused a faster nucleation, but an overall slower growth rate. In this case, PVCap performed more efficiently than PVP in terms of prolonging in nucleation time and controlling growth rate. It is clear that the application of these two KHIs should be reviewed prior to their use under ocean field conditions. In the case of hydrate blockages, our observations that hydrate dissociation started later in the presence of inhibitors and complete dissociation took longer in the presence of inhibitors could have far reaching economic implications for industry.

Acknowledgments

Authors thank Dr. J.D. Lee for providing PVCap for this work. The financial support from the Natural Sciences and Engineering Research Council of Canada (NSERC) is greatly appreciated.

References

[1] Sloan ED, Koh CA. Clathrate hydrates of natural gases. CRC Pressl Llc; 2008.
[2] Davidson DW. Clathrate hydrates. Water cryst. Hydrates aqueous solutions simple nonelectrolytes. Springer; 1973.
[3] Hammerschmidt EG. Formation of gas hydrates in natural gas transmission lines. Ind Eng Chem 1934;26:851–5.
[4] Ellison BT, Gallagher CT, Frostman LM, Lorimer SE. The physical chemistry of wax, hydrates, and asphaltene. In: Offshore Technol Conf, 2000.
[5] Mehta AP, Klomp UC. An industry perspective on the state of the art of hydrates management. In: Fifth Int Conf Gas Hydrates Trondheim; 2005.
[6] Englezos P. Clathrate hydrates. Ind Eng Chem Res 1993;32:1251–74.
[7] Sloan ED. Fundamental principles and applications of natural gas hydrates. Nature 2003;426:353–63.
[8] Creek JL. Efficient hydrate plug prevention. Energy Fuels 2012;26:4112–6.
[9] Lederhos JP, Long JP, Sum A, Christiansen RL, Sloan Jr ED. Effective kinetic inhibitors for natural gas hydrates. Chem Eng Sci 1996;51:1221–9.
[10] Fu B. The development of advanced kinetic hydrate inhibitors. Spec Publ-R Soc Chem 2002;280:264–76.
[11] Fu B, Neff S, Mathur A, Bakeev K. Application of low-dosage hydrate inhibitors in deepwater operations. Old Prod Facil 2002;17:133–7.
[12] Kelland MA. History of the development of low dosage hydrate inhibitors. Energy Fuels 2006;20:825–47.
[13] Lachance JW, Dendy Sloan E, Koh CA. Effect of hydrate formation/dissociation on emulsion stability using DSC and visual techniques. Chem Eng Sci 2008;63:3942–7.
[14] Daraboina N, Moudrakovski IL, Ripmeester JA, Walker VK, Englezos P. Assessing the performance of commercial and biological gas hydrate inhibitors using nuclear magnetic resonance microscopy and a stirred autoclave. Fuel 2012.
[15] Daraboina N, Linga P, Ripmeester J, Walker VK, Englezos P. Natural gas hydrate formation and decomposition in the presence of kinetic inhibitors. 2. Stirred reactor experiments. Energy Fuels 2011;25:4384–91.
[16] Daraboina N, Ripmeester J, Walker VK, Englezos P. Natural gas hydrate formation and decomposition in the presence of kinetic inhibitors. 1. High pressure calorimetry. Energy Fuels 2011;25:4392–7.
[17] Ohno H, Susilo R, Gordienko R, Ripmeester J, Walker VK. Interaction of antifreeze proteins with hydrocarbon hydrates. Chem- Eur J 2010;16:10409–17.
[18] Ohno H, Moudrakovski I, Gordienko R, Ripmeester J, Walker VK. Structures of hydrocarbon hydrates during formation with and without inhibitors. J Phys Chem A 2012;116:1337–43.
[19] Zeng H, Wilson LD, Walker VK, Ripmeester JA. The inhibition of tetrahydrofuran clathrate–hydrate formation with antifreeze protein. Can J Phys 2003;81:17–24.
[20] Anderson BJ, Tester JW, Borghi GP, Trout BL. Properties of inhibitors of methane hydrate formation via molecular dynamics simulations. J Am Chem Soc 2005;127:17852–62.
[21] Davenport JR, Musa OM, Paterson MJ, Piepenbrock M-OM, Fucke K, Steed JW. A simple chemical model for clathrate hydrate inhibition by polyvinylcaprolactam. Chem Commun 2011;47:9891–3.
[22] Lederhos JP, Sloan ED. Transferability of kinetic inhibitors between laboratory and pilot plant. SPE Annu Tech Conf Exhib 1996.
[23] Notz PK, Bumgardner SB, Schaneman BD, Todd JL. Application of kinetic inhibitors to gas hydrate problems. Old Prod Facil 1996;11:256–60.
[24] Dong Lee J, Wu H, Englezos P. Cationic starches as gas hydrate kinetic inhibitors. Chem Eng Sci 2007;62:6548–55.
[25] Lee JD, Englezos P. Enhancement of the performance of gas hydrate kinetic inhibitors with polyethylene oxide. Chem Eng Sci 2005;60:5323–30.
[26] Jensen L, Thomsen K, von Solms N. Inhibition of structure I and II gas hydrates using synthetic and biological kinetic inhibitors. Energy Fuels 2010;25:17–23.
[27] Daraboina N, Ripmeester J, Walker VK, Englezos P. Natural gas hydrate formation and decomposition in the presence of kinetic inhibitors. 3. Structural and compositional changes. Energy Fuels 2011;25:4398–404.
[28] Ohno H, Strobel TA, Dec SF, Sloan J, Koh CA. Raman studies of methane–ethane hydrate metastability. J Phys Chem A 2009;113:1711–6.
[29] Ajiro H, Takemoto Y, Akashi M, Chua PC, Kelland MA. Study of the kinetic hydrate inhibitor performance of a series of poly(N-alkyl-N-vinylacetamide)s. Energy Fuels 2010;24:6400–10.
[30] O'Reilly R, Ieong NS, Chua PC, Kelland MA. Missing poly(N-vinyl lactam) kinetic hydrate inhibitor: high-pressure kinetic hydrate inhibition of structure II gas hydrates with poly(N-vinyl piperidone) and other poly(N-vinyl lactam) homopolymers. Energy Fuels 2011;25:4595–9.
[31] Glenat P, Peytavy J-L, Holland-Jones N, Grainger M. South-pars phases 2 and 3: the kinetic hydrate inhibitor (KHI) experience applied at field start-up. Abu Dhabi Int Conf Exhib 2004.
[32] Ballard AL, Sloan Jr ED. The next generation of hydrate prediction: I. Hydrate standard states and incorporation of spectroscopy. Fluid Phase Equilib 2002;194:371–83.
[33] Linga P, Kumar R, Englezos P. Gas hydrate formation from hydrogen/carbon dioxide and nitrogen/carbon dioxide gas mixtures. Chem Eng Sci 2007;62:4268–76.
[34] Linga P, Haligva C, Nam SC, Ripmeester JA, Englezos P. Recovery of methane from hydrate formed in a variable volume bed of silica sand particles. Energy Fuels 2009;23:5508–16.
[35] Dalmazzone D, Kharrat M, Lachet V, Fouconnier B, Clausse D. DSC and PVT measurements. J Therm Anal Calorim 2002;70:493–505.
[36] Zeng H, Wilson LD, Walker VK, Ripmeester JA. Effect of antifreeze proteins on the nucleation, growth, and the memory effect during tetrahydrofuran clathrate hydrate formation. J Am Chem Soc 2006;128:2844–50.
[37] Wathen B, Kwan P, Jia Z, Walker VK. Modeling the interactions between poly (n-vinylpyrrolidone) and gas hydrates: factors involved in suppressing and accelerating hydrate growth. High Perform Comput Syst Appl 2010:117–33.
[38] Zeng H, Lu H, Huva E, Walker VK, Ripmeester JA. Differences in nucleator adsorption may explain distinct inhibition activities of two gas hydrate kinetic inhibitors. Chem Eng Sci 2008;63:4026–9.
[39] Rodahl M, Höök F, Fredriksson C, Keller CA, Krozer A, Brzezinski P, et al. Simultaneous frequency and dissipation factor QCM measurements of biomolecular adsorption and cell adhesion. Faraday Discuss 1997;107:229–46.

[40] Rodahl M, Hook F, Krozer A, Brzezinski P, Kasemo B. Quartz crystal microbalance setup for frequency and Q-factor measurements in gaseous and liquid environments. Rev Sci Instrum 1995;66:3924–30.
[41] Kumar R, Lee JD, Song M, Englezos P. Kinetic inhibitor effects on methane/propane clathrate hydrate-crystal growth at the gas/water and water/*n*-heptane interfaces. J Cryst Growth 2008;310:1154–66.
[42] Lou A, Pethica BA, Somasundaran P. Interfacial and monolayer properties of poly (vinylcaprolactam). Langmuir 2000;16:7691–3.
[43] Noskov BA, Akentiev AV, Miller R. Dynamic surface properties of poly (vinylpyrrolidone) solutions. J Colloid Interface Sci 2002;255:417–24.
[44] Águila-Hernández J, Trejo A, García-Flores BE. Volumetric and surface tension behavior of aqueous solutions of polyvinylpyrrolidone in the range (288–303) K. J Chem Eng Data 2011;56:2371–8.
[45] Yang J, Tohidi B. Characterization of inhibition mechanisms of kinetic hydrate inhibitors using ultrasonic test technique. Chem Eng Sci 2011;66:278–83.
[46] Lee JD, Englezos P. Unusual kinetic inhibitor effects on gas hydrate formation. Chem Eng Sci 2006;61:1368–76.
[47] Makogon YF, Holditch SA. Lab work clarifies gas hydrate formation, dissociation. Oil Gas J 2001;99:47.
[48] Ballard AL, Sloan Jr ED. Hydrate phase diagrams for methane + ethane + propane mixtures. Chem Eng Sci 2001;56:6883–95.
[49] Davies SR, Hester KC, Lachance JW, Koh CA, Dendy Sloan E. Studies of hydrate nucleation with high pressure differential scanning calorimetry. Chem Eng Sci 2009;64:370–5.